Proceedings of the 1998 IEEE
International Conference on Robotics & Automation
Leuven, Belgium • May 1998

# Frequency Modulation In Anthropomorphic Robots With Kinematic And Force Redundancies

**Byung-Ju Yi[1], Sang-Rok Oh[2], Il Hong Suh[3], Whee Kuk Kim[4]**
[1]Dept. of Control & Instrumentation Eng., Hanyang Univ. Korea
[2]Div. of Electronics and Information Tech. KIST, Korea
[3]Dept. of Electronics Eng., Hanyang Univ. Korea
[4]Dept. of Control & Instrumentation Eng., Hanyang Univ. Korea

***Abstract***

*Typical biomechanical systems such as human body and mammals possess abundant muscles which are more than required for motion generation of such systems. The purpose of this work is to verify a biological phenomenon, the so called frequency modulation, in a mathematical manner. The frequency modulation represents a simultaneous control of force and kinematic redundancies. The phenomenon of frequency modulation is explained through a human-like anthropomorphic robot. A load distribution method for frequency modulation via redundant actuation is also introduced. To show the effectiveness of the proposed algorithms, several simulation results are illustrated.*

## *1. Introduction*

*Mobility* ( $M$) of a system is defined as the number of independent variables which must be specified in order to locate its elements relative to another. When $M$ is greater than the degree-of-freedom of the operational (or task) space, the system is called *a kinematically redundant system*[1-10]. On the other hand, when the number of actuators is greater than $M$ (this situation usually happens in closed-chain linkage systems), the system is called *redundantly actuated* For instance, five-bar mechanisms require at least two actuators (that is, $M=2$) to control the motion at the end-point. When this mechanism is driven by more than two actuators for the same motion generation, the system becomes redundantly actuated. General biomechanical systems including the human body as well as the bodies of mammals and insects are redundantly actuated. For example, mobility of the human upper-extremity (arm) shown in Figure 1 has 6 human actuators (i.e., muscles)[4], while mobility of this system is two. Accordingly, it has 4 redundant actuators. Now, a question may arise for the necessity of those hyper-redundant actuators. Hogan [12] explained the existence of the hyper-redundant muscles of the human body in terms of the spring-like impedance property. Since the neural feedback control of dynamic behaviour is severely curtailed by the inevitable time delays associated with the neural transmission, neural feedback is only effective below a certain frequency. Thus, he mentioned that synergistic activation of antagonistic muscles might be a single unified approach for controlling dynamic interaction at all frequencies. Conclusively, the spring-like impedance property comes from the antagonistic activation of hyper-redundant muscles. He also pointed out that the inertia property could be another important impedance property. Since the inertia property at the end-point of the human arm is a function of the joint angles of the system, the human arm with kinematically redundant structure is able to modulate the inertia property by its self-motion without changing the end-position of the arm. The damping impedance property is also a function of the joint angles, and thus modulation of the damping impedance is similar to that of the inertia property. Inspired by those ideas stemming from the biomechanics research fields, Yi and Freeman [1] proposed a general methodology for actively adjustable springs, and conditions for actively adjustable springs are derived for general redundantly actuated closed-chain mechanisms. Also, they successfully applied those conditions to the analysis of redundantly actuated linkage systems [2, 3, 6] and some of the biomechanical models in terms of the spring-like impedance property[5]. However, previous research was restricted to analysis of kinematically nonredundant structures such as five-bar mechanisms.

In this work, we will consider a kinematically redundant anthropomorphic robotic mechanism as shown in Fig. 2, which only controls the x- and y-directional motions at the task space. The system is driven by six linear actuators around the first- and the second-joints and one rotary actuator at the third joint. In this case, the effective inertia property at the task point can be controlled by self-motion at the joint space.

The organization of this paper is as follows : Initially, we introduce the kinematic and dynamic modeling methodology for the proposed anthropomorphic robotic mechanism, in section 2. In section 3, the frequency modulation algorithm and the associated load distribution algorithm will be proposed. In section 4, the effectiveness of the of frequency modulation is proven through simulation. Finally, we draw conclusions.

0-7803-4300-x-5/98 $10.00 © 1998 IEEE

## 2. Kinematic Modeling

The modeling methodology integrates the Generalized Principle of D'Alembert with the method of kinematic influence coefficients(*KIC*) resulting in closed form vector expressions[11].

### 2.1 Open-chain kinematics

Assume that a closed-chain mechanism consists of $R$ chains. Adopting the standard Jacobian representation for the velocity of a vector of $N$ dependent (output) parameters $\boldsymbol{u}$ in terms of a set of $M$ independent input coordinates ${}_r\dot{\boldsymbol{\theta}}$ of $r$*th* open-chain, one has

$$\dot{\boldsymbol{u}} = [\,{}_rG_\theta^u\,]\;{}_r\dot{\boldsymbol{\theta}}_a. \tag{1}$$

Here,

$$[\,{}_rG_\theta^u\,] = [\,\frac{\partial u}{\partial {}_r\theta_1}\,,\frac{\partial u}{\partial {}_r\theta_2}\,,\cdots,\frac{\partial u}{\partial {}_r\theta_N}\,] \tag{2}$$

is the Jacobian relating the coordinates $\boldsymbol{u}$ and ${}_r\dot{\boldsymbol{\theta}}$ and is of dimension of $N\times M$. Generally, the acceleration vector $\ddot{\boldsymbol{u}}$ of a set of $N$ dependent parameters $\boldsymbol{u}$ is represented in terms of the $M$ independent coordinates $\boldsymbol{\phi}$ as

$$\ddot{\boldsymbol{u}} = [\,{}_rG_\theta^u\,]\;{}_r\ddot{\boldsymbol{\theta}} + {}_r\dot{\boldsymbol{\theta}}^T[\,{}_rH_{\theta\theta}^u\,]\;{}_r\dot{\boldsymbol{\theta}}, \tag{3}$$

where the second-order *KIC* array $[\,{}_rH_{\theta\theta}^u\,]$ is of dimension of $N\times M\times M$, and the $i$*th* plane of $[\,{}_rH_{\theta\theta}^u\,]$, $[\,{}_rH_{\theta\theta}^u\,]_{i;;}$ with dimension of $M\times M$ is defined as

$$[\,{}_rH_{\theta\theta}^u\,]_{i;;} = \left[\frac{\partial^2 u_i}{\partial {}_r\boldsymbol{\theta}\,\partial {}_r\boldsymbol{\theta}}\right]. \tag{4}$$

### 2.2 Internal kinematics for six closed-chains

Consider a human-like anthropomorphic robotic manipulator shown in Fig. 2. This system has two typical features. As the first feature, it has six closed-kinematic chain as shown in Fig. 3. As the second feature, this system has one kinematic redundancy. Since the mobility of this mechanism is given as three, three actuators are minimally required to control the mechanism. However, we assume that all linear actuators are activated.

For the six closed-chains, internal kinematic relationships between the dependent joints and the independent joints is required to deal with our further analysis of the given robotic mechanism. Specifically, consider the second five-bar of Fig. 3. Note that the two open-chains of the 5-bar mechanism have a common kinematic relation at the end-location $(x, y)$ of the linear actuator $d_3$. Then, the kinematic constraint equations are written by

$$x = l_1c_1 + b_1c_{12} = a_1 + d_2\,c_5, \tag{5}$$

$$y = l_1s_1 + b_1s_{12} = d_2\,s_5. \tag{6}$$

Differentiating Eqs. (5) and (6) with respect to time, the equivalent velocity and acceleration relations are, respectively, given by

$$[\,{}_1G_\theta^u\,]\;{}_1\dot{\boldsymbol{\theta}} = [\,{}_2G_\theta^u\,]\;{}_2\dot{\boldsymbol{\theta}}, \tag{7}$$

and

$$[\,{}_1G_\theta^u\,]\;{}_1\ddot{\boldsymbol{\theta}} + {}_1\dot{\boldsymbol{\theta}}^T[\,{}_1H_{\theta\theta}^u\,]\;{}_1\dot{\boldsymbol{\theta}} = [\,{}_2G_\theta^u\,]\;{}_2\ddot{\boldsymbol{\theta}} + {}_2\dot{\boldsymbol{\theta}}^T[\,{}_2H_{\theta\theta}^u\,]\;{}_2\dot{\boldsymbol{\theta}}, \tag{8}$$

where $[\,{}_1G_\theta^u\,]$ and $[\,{}_2G_\theta^u\,]$, respectively, imply the Jacobians of the first and second open-chain, and $[\,{}_1H_{\theta\theta}^u\,]$ and $[\,{}_2H_{\theta\theta}^u\,]$ denote the Hessian arrays of the first and second open-chain of the system.

Selecting the joints $\theta_1$ and $\theta_2$ as the independent joints ( $\boldsymbol{\theta}_a$) and the joints $\theta_5$ and $d_3$ as the dependent joints ( $\boldsymbol{\theta}_p$), Eq. (8) can be rewritten as

$$[A]\;\ddot{\boldsymbol{\theta}}_p = [B]\;\ddot{\boldsymbol{\theta}}_a, \tag{9}$$

where

$$[A] = [\,{}_2G_\theta^u\,], \tag{10}$$

$$[B] = [\,{}_1G_\theta^u\,], \tag{11}$$

$$\dot{\boldsymbol{\theta}}_a = \begin{pmatrix}\dot\theta_1\\ \dot\theta_2\end{pmatrix},\quad \dot{\boldsymbol{\theta}}_p = \begin{pmatrix}\dot\theta_5\\ \dot d_3\end{pmatrix}. \tag{12}$$

Now, premultiplying the inverse of the matrix [A] to both sides of Eq. (9) yields

$$\dot{\boldsymbol{\theta}}_p = [\,G_a^p\,]\;\dot{\boldsymbol{\theta}}_a, \tag{13}$$

where $[\,G_a^p\,]_{2\times 2}$ denotes the first-order *KIC* matrix relating $\dot{\boldsymbol{\theta}}_p$ to $\dot{\boldsymbol{\theta}}_a$.

Now, the velocity of the linear actuator is extracted from Eq. (14) as follows

$$\dot d_2 = [\,G_a^p\,]_{2:}\;\dot{\boldsymbol{\theta}}_a, \tag{14}$$

where $[\,G_a^p\,]_{2:}$ denotes the *2nd* row of $[\,G_a^p\,]$. The same procedure is applied to the rest of the closed-chains to obtain the relationship similar to Eq. (14). Finally, the relationship between the independent joints and the six linear joints is constructed as

$$\dot{\boldsymbol{d}} = [\,G_a^d\,]\;\dot{\boldsymbol{\theta}}_a, \tag{15}$$

where

$$\dot{\boldsymbol{d}} = (\,\dot d_1\;\;\dot d_2\;\;\dot d_3\;\;\dot d_4\;\;\dot d_5\;\;\dot d_6\,)^T \tag{16}$$

and

$$[\,G_a^d\,]^T = \begin{bmatrix} g_1^{d1} & g_1^{d2} & g_1^{d3} & g_1^{d4} & 0 & 0\\ g_2^{d1} & g_2^{d2} & 0 & 0 & g_2^{d5} & g_2^{d6}\end{bmatrix}^T. \tag{17}$$

In Eq. (17), $g_i^{dj}$ denotes $\dfrac{\partial d_j}{\partial \theta_i}$.

The second-order, three-dimensional *KIC* array $[\,H_{aa}^d\,]_{6\times 2\times 2}$ relating $\ddot{\boldsymbol{d}}$ to $\ddot{\boldsymbol{\theta}}_a$ can be easily obtained in a similar manner as follows [1] :

$$\ddot{\boldsymbol{d}} = [\,G_a^d\,]\;\ddot{\boldsymbol{\theta}}_a + \dot{\boldsymbol{\theta}}_a^T[\,H_{aa}^d\,]\;\dot{\boldsymbol{\theta}}_a. \tag{18}$$

Also, $[\,H_{aa}^d\,]$ is defined as

$$[H_{aa}^{d}]_{1;:}=\begin{bmatrix} h_{11}^{d1} & h_{12}^{d1} \\ h_{12}^{d1} & h_{22}^{d1} \end{bmatrix},\quad [H_{aa}^{d}]_{2;:}=\begin{bmatrix} h_{11}^{d2} & h_{12}^{d2} \\ h_{12}^{d2} & h_{22}^{d2} \end{bmatrix},$$

$$[H_{aa}^{d}]_{3;:}=\begin{bmatrix} h_{11}^{d3} & 0 \\ 0 & 0 \end{bmatrix},\quad [H_{aa}^{d}]_{4;:}=\begin{bmatrix} h_{11}^{d4} & 0 \\ 0 & 0 \end{bmatrix},$$

$$[H_{aa}^{d}]_{5;:}=\begin{bmatrix} 0 & 0 \\ 0 & h_{22}^{d5} \end{bmatrix},\quad [H_{aa}^{d}]_{6;:}=\begin{bmatrix} 0 & 0 \\ 0 & h_{22}^{d6} \end{bmatrix}, \quad (19)$$

where

$$h_{ij}^{dk}=\frac{\partial^2 d_k}{\partial\theta_i\partial\theta_j}. \quad (20)$$

According to the duality between the velocity vector and force vector, the force relation between the independent joints and the linear joints is described by

$$\boldsymbol{T}_a = [G_a^d]^T \boldsymbol{F}_d, \quad (21)$$

where

$$\boldsymbol{T}_a=(T_1\ T_2)^T,\ \boldsymbol{F}_d=(F_1\ F_2 F_3 F_4 F_5 F_6)^T. \quad (22)$$

Then, when activating all linear actuators, the effective load referenced to the independent joints is expressed by

$$\boldsymbol{T}_a^* = \boldsymbol{T}_a + [G_a^d]^T \boldsymbol{F}_d = [G_a^d]^T \boldsymbol{F}_d, \quad (23)$$

where $\boldsymbol{T}_a$ is equal to zero vector since the independent joints are passive joints.

### *2.3 Forward Kinematics*

For the system given in Fig. 2, three revolute joints $\theta_1$, $\theta_2$, and $\theta_3$ have been decided as the independent joints. If only the output positions are vector is controlled, they are given in terms of the independent input vector as follows

$$x = l_1c_1 + l_2c_{1+2} + l_3c_{1+2+3}, \quad (24)$$

$$y = l_1s_1 + l_2s_{1+2} + l_3s_{1+2+3}. \quad (25)$$

Now, the first-order forward kinematics is obtained as

$$\dot{\boldsymbol{u}} = [G_a^u]\,\dot{\boldsymbol{\theta}}_a, \quad (26)$$

where the dimension of $[G_a^u]$ is $2\times3$. One kinematic redundancy existing in the joint space can be employed to change the kinematic and dynamic characteristics. In the following discussion, we employ the kinematic redundancy to adjust the inertia property at the task space by changing the manipulator configuration. The second-order forward kinematic array $[H_{aa}^u]$ is also straightforward [11].

### *2.4 Dynamic modeling for anthropomorphic manipulator*

We assume that the last revolute joint is locked once a desired manipulator configuration is achieved. In that case, the dimension of $[G_a^u]$ becomes $2\times2$ by extracting the third column of itself. Then, the inverse of $[G_a^u]$ (i.e., $[G_u^a]$) from Eq. (26) is uniquely decided.

Using the principle of virtual work, the generalized inertial loads of an $M$-link open-chain as referenced to the M relative joint parameters are given as [11]

$$_r\boldsymbol{T}_\theta = [{}_rI_{\theta\theta}^*]\,{}_r\ddot{\boldsymbol{\theta}} + {}_r\dot{\boldsymbol{\theta}}^T[{}_rP_{\theta\theta\theta}^*]\,{}_r\dot{\boldsymbol{\theta}},\ (r=1-6) \quad (27)$$

where $[{}_rI_{\theta\theta}^*]$ and $[{}_rP_{\theta\theta\theta}^*]$ denote the effective inertia matrix and the inertia power array, respectively.

Now, employing the principle of virtual work, the open-chain dynamics can be directly incorporated into closed-chain dynamics according to

$$\boldsymbol{T}_\theta^T\,\delta\boldsymbol{\theta} = \boldsymbol{T}_a^T\,\delta\boldsymbol{\theta}_a. \quad (28)$$

The total system dynamics is obtained using Eqs. (27) and (28) as follows :

$$\begin{aligned}\boldsymbol{T}_a^* &= [G_a^\theta]^T\boldsymbol{T}_\theta \\ &= [I_{aa}^*]\,\ddot{\boldsymbol{\theta}}_a + \dot{\boldsymbol{\theta}}_a^T[P_{aaa}^*]\,\dot{\boldsymbol{\theta}}_a, \end{aligned} \quad (29)$$

where the inertial matrix $[I_{aa}^*]$ and inertia power array $[P_{aaa}^*]$ defined in the independent joint set are given by

$$[I_{aa}^*] = \sum_{r=1}^{2}[{}_rG_a^\theta]^T[{}_rI_{\theta\theta}^*][{}_rG_a^\theta], \quad (30)$$

$$\begin{aligned}[P_{aaa}^*] = \sum_{r=1}^{2}\{&([{}_rG_a^\theta]^T[{}_rI_{\theta\theta}^*])o[{}_rH_{aa}^\theta] \\ &+[{}_rG_a^\theta]^T([{}_rG_a^\theta]^T o[{}_rP_{\theta\theta\theta}^*])[{}_rG_a^\theta]\}, \end{aligned} \quad (31)$$

and $[{}_rG_a^\theta]$ and $[{}_rH_{aa}^\theta]$, respectively, denote the first-order and the second-order kinematic influence coefficient matrices relating the joints of *rth* serial chain to the independent joints of the system.

Now, the dynamic formulation with respect to the output(task or operational) coordinates is obtained by employing the coordinate transformation technique between the minimum coordinates and the task coordinates :

$$\boldsymbol{T}_u = [I_{uu}^*]\,\ddot{\boldsymbol{u}} + \dot{\boldsymbol{u}}^T[P_{uuu}^*]\,\dot{\boldsymbol{u}}, \quad (32)$$

where

$$[I_{uu}^*] = [G_u^a]^T[I_{aa}][G_u^a], \quad (33)$$

$$\begin{aligned}[P_{uuu}^*] = &[G_u^a]^T([G_u^a]^T o[P_{aaa}])[G_u^a] \\ &+([G_u^a]^T[I_{aa}])o[H_{uu}^a] \end{aligned} \quad (34)$$

and $\boldsymbol{T}_u$ denotes the load vector at the output position, and $[I_{uu}^*]$, $[P_{uuu}^*]$ represent the inertial matrix, inertia power array defined in the output position, respectively.

## *3. Feedforward Frequency Modulation*

### *3.1 Frequency modeling*

In a state of static equilibrium, Eq. (23) can be described by

$$\boldsymbol{T}_a^* = [G_a^d]^T\boldsymbol{F}_d = 0. \quad (35)$$

Given a disturbance to the system under force equilibrium, a spring-like behaviour occurs to the system. Assuming that the magnitude of $\boldsymbol{F}_d$ remains constant, the effective stiffness matrix $[K_{aa}]$ with respect to the independent coordinates is obtained by differentiating Eq. (35) with respect to the independent coordinate set $\boldsymbol{\theta}_a$ [1]

$$[K_{aa}] = (-\boldsymbol{F}_d)^T o[H_{aa}^d]^T, \quad (36)$$

where $[H_{aa}^d]$ is given in Eq. (19). Noting that the stiffness relationship between the output coordinates and the independent coordinates is given by

$$[K_{uu}] = [G_u^a]^T[K_{aa}][G_u^a], \quad (37)$$

substituting Eq. (36) into Eq. (37) yields the following stiffness matrix expressed with respect to the output space

$$[K_{uu}] = (-\boldsymbol{F}_d)^T o [H_{uu}^d] , \quad (38)$$

where

$$[H_{uu}^d] = [G_u^a]^T[H_{aa}^d][G_u^a] . \quad (39)$$

Given a small displacement to the system in a state of static equilibrium ( $\dot{\boldsymbol{u}} = 0$), the dynamic equation of the system is given, from Eq. (40), as

$$[I_{uu}^*]\,\delta\ddot{\boldsymbol{u}} = \boldsymbol{T}_u , \quad (40)$$

where

$$\boldsymbol{T}_u = \Delta([G_u^d]^T \boldsymbol{F}_d) = (\boldsymbol{F}_d{}^T o [H_{uu}^d]^T)\delta\boldsymbol{u} . \quad (41)$$

The above equation is rearranged as

$$[I_{uu}^*]\,\delta\ddot{\boldsymbol{u}} + [K_{uu}]\,\delta\boldsymbol{u} = 0 , \quad (42)$$

where $[K_{uu}]$ is the stiffness matrix given in Eq. (38). Premultiplying $[I_{uu}^*]^{-1}$ to both sides of Eq. (43) yields

$$\delta\ddot{\boldsymbol{u}} + [I_{uu}^*]^{-1}[K_{uu}]\,\delta\boldsymbol{u} = 0 , \quad (43)$$

where the frequency matrix $[w_{uu}]$ is defined according to

$$[w_{uu}][w_{uu}]^T = [I_{uu}^*]^{-1}[K_{uu}] = (-\boldsymbol{F}_d)^T o ([I_{uu}^*][H_{uu}^d]) . \quad (44)$$

Since the frequency matrix is diagonal, Eq. (44) can be written in a matrix form

$$\boldsymbol{w}_u = [W_u^d]\boldsymbol{F}_d , \quad (45)$$

where $\boldsymbol{w}_u$ and $[W_u^d]$ are defined as

$$\boldsymbol{w}_u = \begin{bmatrix} w_{xx}^2 \\ w_{xy}^2 \\ w_{yy}^2 \end{bmatrix} = \begin{bmatrix} [w_{uu}]_{1:1}^2 \\ [w_{uu}]_{1:2}[w_{uu}]_{1:2}^T \\ [w_{uu}]_{2:2}^2 \end{bmatrix} \quad (46)$$

and

$$[W_u^d] = \begin{bmatrix} \{[I_{uu}^*]^{-1}([G_u^a]^T[H_{aa}^d][G_u^a])\}_{:1:1} \\ \{[I_{uu}^*]^{-1}([G_u^a]^T[H_{aa}^d][G_u^a])\}_{:1:2} \\ \{[I_{uu}^*]^{-1}([G_u^a]^T[H_{aa}^d][G_u^a])\}_{:2:2} \end{bmatrix} . \quad (47)$$

### *3.2 Load Distribution Algorithm*

Yi and Freeman[1] derived necessary conditions for stiffness modulation by antagonistic preloading in redundantly actuated systems. According to those conditions, a planar closed-chain system having one closed-loop has two nonlinear constraint equations, which allows modulation of the same number of stiffness elements at least. Since the anthropomorphic manipulator has six independent closed-chains, twelve nonlinear holonomic equations satisfies full modulation of three stiffness elements (that is, $k_{xx}$, $k_{xy}$, and $k_{yy}$) in the task space.

Note that the frequency matrix is nothing but a stiffness matrix weighted by the inertia matrix as seen from Eq. (44). Therefore, three components (that is, $\omega_{xx}$, $\omega_{xy}$, and $\omega_{yy}$) of $\boldsymbol{w}_u$ vector can be independently controlled. In regard of the number of actuators, at least, five actuators are necessary to control the motion in the x- and y-directions and the three frequency components. In simulation, the magnitudes of $\omega_{xx}$, $\omega_{xy}$, and $\omega_{yy}$ are to be controlled simultaneously under static equilibrium.

Now, in order to modulate the desired $\boldsymbol{w}_u$ in static equilibrium, a load distribution method is introduced in this section. Initially, combine Eqs. (35) and (45) in a matrix form, given by

$$\begin{bmatrix} [G_a^d]^T \\ -[W_u^d] \end{bmatrix} \boldsymbol{F}_d = \begin{bmatrix} 0 \\ \boldsymbol{w}_u \end{bmatrix} . \quad (48)$$

Then, the general solution of Eq. (48) is described by

$$\boldsymbol{F}_d = [G_{com}]^+ \boldsymbol{a} + ([I] - [G_{com}]^+[G_{com}])\boldsymbol{\varepsilon}, \quad (49)$$

where $[G_{com}]^+$ denotes a pseudo-inverse solution of $[G_{com}]$, and $[G_{com}]$ and $\boldsymbol{a}$ are given as

$$[G_{com}] = \begin{bmatrix} [G_a^d]^T \\ -[W_u^d] \end{bmatrix} \quad (50)$$

and

$$\boldsymbol{a} = \begin{bmatrix} 0 \\ \boldsymbol{w}_u \end{bmatrix} . \quad (51)$$

Also, the second-term of Eq. (49) represents a homogeneous solution which creates an internal loading. This internal loading can be utilized for additional subtasks.

## *4. Simulation*

The oscillation of the anthropomorphic manipulator with respect to a desired position can be achieved by activating the system actuators such that the system has the desired frequency characteristics at the equilibrium position, with the initial position of the end-point being deviated from the equilibrium position by the amount of the desired amplitude of oscillation. One kinematic redundancy can be utilized to change the configuration(i.e., self-motion) at the same task position, which is required to avoid obstacles or change the inertia property at the task position which enables the modulation of the motion frequency of the system in a more active manner since the inertia property can be possibly modulated by the self-motion using the kinematic redundancy of the kinematically redundant structure. Here, we assume that the last revolute joint is locked once a desired manipulator configuration is achieved.

The kinematic and dynamic parameters for the anthropomorphic manipulator are given by

$$l_1 = 0.2m, \quad l_2 = 0.1m, \quad l_3 = 0.05m$$

$$a_1 = a_2 = 0.1\ m, \ a_3 = a_5 = 0.2m$$

$$a_4 = a_6 = 0.15m$$

$b_1 = b_2 = b_4 = b_5 = 0.01m$, $b_3 = 0.1\,m$,
$b_6 = 0.2m$
$m_1 = 0.5\,kg \quad m_2 = 0.3\,kg \quad m_3 = 0.1\,kg$
$I_{z1} = 0.0017\,kg \cdot m^2 \quad I_{z2} = 0.00056\,kg \cdot m^2$
$I_{z3} = 0.000021\,kg \cdot m^2$, (52)

where the origin and insertion points for each linear actuator are determined based on the observation of the structure of the human upper extremity.

Given an initial displacement to the x-direction by 1 $cm$, Fig. 4 shows the vibration response about a equilibrium position $(x,\ y) = (0.1\ 0.15)$ m with a hand orientation $\Phi = -90^\circ$. In this simulation, $\omega_{xy}$ is modulated as zero, and $\omega_{xx}$ and $\omega_{yy}$ are modulated identically as 4 rad/sec steadily. On the other hand, Fig. 5 shows the vibration response about the same equilibrium position $(x,\ y) = (0.1\ 0.15)$ m and the same frequency modulation with a different hand orientation $\Phi = -45^\circ$. A slight oscillation in the y direction is observed. It tells us that the amount of dynamic coupling between the x- and y-directions depends upon the manipulator configuration. Therefore, in order to use the frequency modulator in a wide range of workspace, an optimization procedure to maximize the frequency modulation throughout the workspace should be performed.

Now, Fig. 6 illustrates the frequency modulation with doubled magnitude of the motion frequency. Just as expected, the frequency content of Fig. 6 is two times of that of Fig. 4 and 5.

It is remarked that frequency modulation will be useful in several complex assembly applications. For example, a certain assembly work such as peg-in-hole problem can be easily performed by inducing vibration to the grasped object. Also, the concept of frequency modulation can be employed for virtual trajectory planning. The spring-like property coupled with the inertia of the human body defines the property of frequency content. Thus, a certain frequency content of the system behaviour is directly converted to the spring-like property. It has been mentioned [12] that modulation of the spring-like property could be employed to produce movement of the system. The production of the movement can be accomplished by a progressive movement of the equilibrium position, which is called a virtual trajectory. The principle significance of the virtual trajectory is that it implies a drastic reduction in the computational effort required to obtain the inverse dynamics for movement generation of robot manipulators. Besides, the applications of motion frequency modulation will be diverse, which will be a future research topic.

## 5. Conclusions

Typical bio-systems are known to have abundant actuators. In this work, we investigate an anthropomorphic robotic manipulator which has the human-like musculoskeletal structure driven by abundant redundant actuators. The phenomenon of actively adjustable frequency modulation is explained through the example model. The concept of the frequency modulation has been presumed by biomechanics area., but has not been mathematically formulated yet. Possible applications of frequency modulator can be found in robotic fields, which needs to be further investigated. We believe that exploration of existing biological systems provides us with many beneficial ideas in the design and control of advanced robotic systems.


## Acknowledgement

This work has been supported by Korean National Science Foundation.


## References


[1] Yi, B-J. and Freeman, R.A., Geometric analysis of antagonistic stiffness in redundantly actuated parallel mechanisms. *Special Issues on Parallel Closed-Chain Mechanism, Journal of Robotic systems* **Vol. 10**, 581-603 (1993).

[2] Yi, B-J., Suh, I.H., and Oh, S-R., Analysis of a five-bar finger mechanism having redundant actuators with applications to stiffness and frequency modulation. *IEEE Proceeding on Robotics and Automation Conference*, (1997).

[3] Yi, B-J., Oh, S-R., and Suh, I.H., Synthesis of actively adjustable frequency modulators : The case for a five-bar finger mechanism. *IEEE/RSJ Proceeding on IROS*, (1997).

[4] Spence, P.A., *Basic human anatomy*. The Benjamin/Cummings Publishing Co. Inc. (1986).

[5] Yi, B-J. and Freeman, R.A., Feedforward spring-like impedance modulation in human arm models, *IEEE Proceeding on Robotics and Automation Conference*, pp. 3121-3128, (1995).

[6] Yi, B-J. and Freeman, R.A,. Synthesis of actively adjustable springs by antagonistic redundant actuation. *Trans. of the ASME, Journal of Dynamic Systems, Measurement, and Controls*, **Vol. 114**, pp. 454-461, (1992).

[7] Nakamura, Y. and Ghodoussi, M., Dynamic computation of closed-link robot mechanisms with nonredundant and redundant actuators. *IEEE Journal of Robotics and Automation* **Vol. 5**, 294-302 (1989).

[8] Nahon, M.A. and Angeles, J., Force optimization in redundantly-actuated closed kinematic chains. *IEEE Proceeding on Robotics and Automation Conference*, pp. 951-956 (1989).

[9] Kumar, V.J. and Gardner, J., Kinematics of redundantly actuated closed chain. *IEEE Journal of Robotics and Automation* **Vol. 6**, 269-273 (1990).

[10] Kurz, R. and Hayward, W., Multiple-goal kinematic optimization of a parallel spherical mechanism with actuator redundancy. *IEEE Journal of Robotics and Automation* **Vol. 8**, 644-651 (1992).

[11] Freeman, R.A. and Tesar, D., Dynamic modeling of serial and parallel mechanisms/robotic systems, Part I-Methodology, Part II-Applications, Proc. of 20th ASME Mechanisms Conference, Orlando, FL, (1988).

[12] Hogan, N., Impedance Control : An approach to manipulation : Part I - Theory, Part II : Implementation, Part III - Applications, J. of Dynamic Systems, Measurement, and Control, **Vol. 107**, pp. 1-24, (1985).

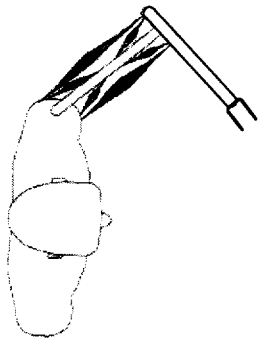

Figure 1 : Human Upper Extremity

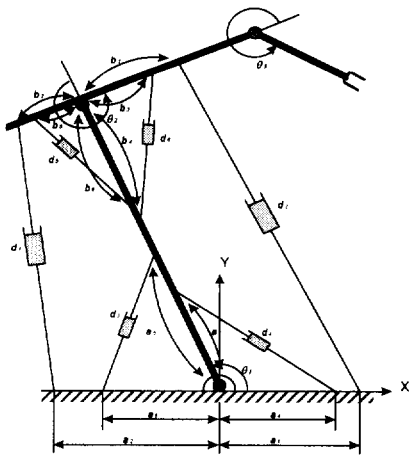

Figure 2 : Anthropomorphic Robot

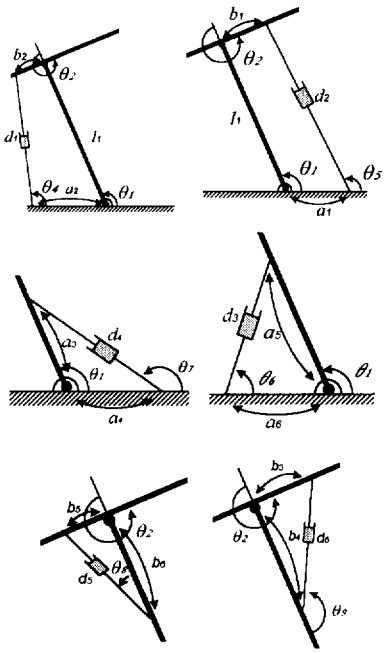

Figure 3 : Six Closed-chains

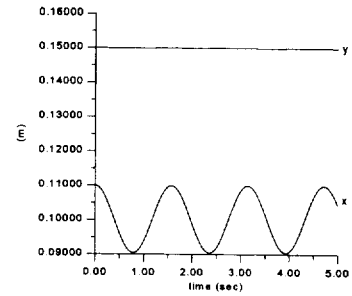


Figure 4 : Frequency Modulation
( $\Phi = -90^{o}$ , $\omega_{xx} = \omega_{yy} = 4\,rad/s$, $\omega_{xy} = 0\,rad/s$ )

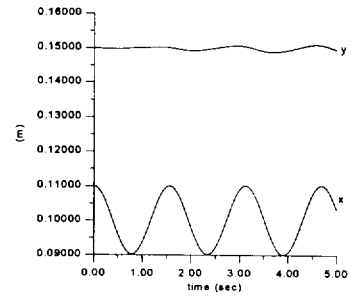


Figure 5 : Frequency Modulation
( $\Phi = -45^{o}$ , $\omega_{xx} = \omega_{yy} = 4\,rad/s$, $\omega_{xy} = 0\,rad/s$ )

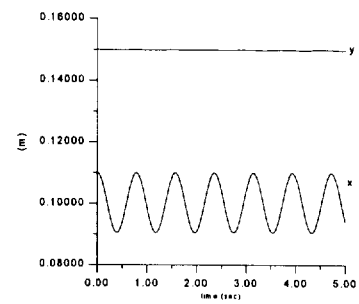


(a) $\Phi = -90^{o}$

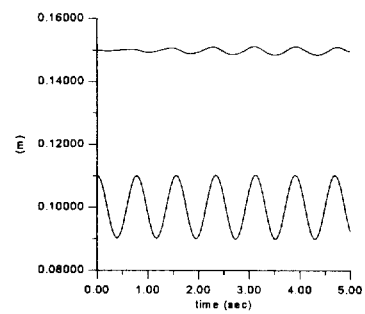


(b) $\Phi = -45^{o}$

Figure 6 : Frequency Modulation
( $\omega_{xx} = \omega_{yy} = 8\,rad/s$, $\omega_{xy} = 0\,rad/s$ )